Readout Sweet Spots for Spin Qubits with Strong Spin-Orbit Interaction

Domonkos Svastits,[1,2] Bence Hetényi,[3] Gábor Széchenyi,[4] James Wootton,[3,5] Daniel Loss,[6] Stefano Bosco,[7] and András Pályi[1,8]

[1]Department of Theoretical Physics, Institute of Physics, Budapest University of Technology and Economics, Műegyetem rakpart 3., H-1111 Budapest, Hungary
[2]Qutility @ Faulhorn Labs, Budapest, Hungary
[3]IBM Research Europe—Zurich, Säumerstrasse 4, 8803 Rüschlikon, Switzerland
[4]ELTE Eötvös Loránd University, Institute of Physics, H-1117 Budapest, Hungary
[5]Moth Quantum AG, Schorenweg 44B, 4144, Arlesheim, Switzerland
[6]Department of Physics, University of Basel, Klingelbergstrasse 82, CH-4056 Basel, Switzerland
[7]QuTech and Kavli Institute of Nanoscience, Delft University of Technology, Delft, The Netherlands
[8]HUN-REN-BME-BCE Quantum Technology Research Group, Műegyetem rakpart 3., H-1111 Budapest, Hungary

(Received 24 June 2025; revised 12 November 2025; accepted 26 January 2026; published 16 March 2026)

Qubit readout schemes often deviate from ideal projective measurements, introducing critical issues that limit quantum computing performance. In this Letter, we model charge-sensing-based readout for semiconductor spin qubits in double quantum dots, and identify key error mechanisms caused by the backaction of the charge sensor. We quantify how the charge noise of the sensor, residual tunneling, and g-tensor modulation degrade readout fidelity, induce a mixed postmeasurement state, and cause leakage from the computational subspace. For state-of-the-art systems with strong spin-orbit interaction and electrically tunable g tensors, we identify a readout sweet spot, that is, a special device configuration where readout is closest to projective. Our framework provides a foundation for developing effective readout error mitigation strategies, with broad applications for optimizing readout performance for a variety of charge-sensing techniques, advancing quantum protocols, and improving adaptive circuits for error correction.

DOI: 10.1103/4x97-np1f

Introduction—Spin qubits confined in semiconductor quantum dots [1] are frontrunners for large-scale quantum computers [2–9]. Their small size, scalability [5,10–13], tunability, CMOS compatibility [14–22], and demonstrated high-fidelity operations [23–25] and readout [26] make them particularly attractive.

A key component of quantum computers is readout, an essential benchmark of which is readout fidelity. However, while experiments demonstrate increasingly high fidelities [22,27–30], this is not the only relevant benchmark [31,32]. Improving other metrics of midcircuit measurements [33–37], such as the quality of the postmeasurement state, and readout-induced leakage [38–41], are key requirements for quantum error correction [42,43] and other dynamic circuits. [44–49]

We present ways to simultaneously improve different metrics of state-of-the-art spin qubit readout. Our model focuses on widely used measurements via Pauli blockade spin-to-charge conversion [50–52] and charge sensing in a double quantum dot (DQD) [53–56]. By modeling charge sensing via a dc-biased quantum point contact (QPC) [57–61], we show that high-fidelity and backaction-free readout requires switching off the interdot tunnel coupling upon charge sensing.

In current devices with strong spin-orbit interaction (e.g., holes in Ge and Si), the fluctuating electric field induced by the carriers of the QPC modulates the g tensors of the spins in the DQD. We show that this modulation influences the readout quality, depending on the static homogeneous magnetic field applied to the DQD. We identify a readout sweet spot, i.e., a specific device configuration where the detrimental backaction effects of the g-tensor modulation are minimized: leakage is suppressed and the purity of the postmeasurement state is maintained. We argue that this readout sweet spot exists universally, independent of spin-orbit interaction details. Our findings provide practical guidelines for high-quality spin-qubit readout.

Model—To describe the readout of a qubit defined in a DQD, we rely on the general framework of quantum measurements, where the *system* is measured indirectly through a *meter* [62,63]. Simplifying earlier approaches [64,65], we use a model in which the meter (the QPC) is represented by a qubit, hence we call it the Qubit Measures Qubit (QMQ) model. To illustrate the harmful effect of residual tunneling in the DQD, we use the model to describe charge qubit readout. Then, we generalize the QMQ model to the readout of spin qubits, where a residual tunneling has

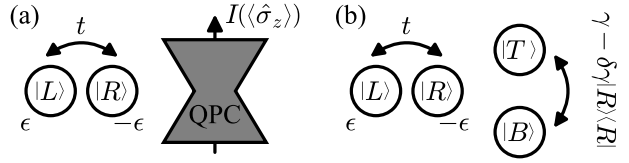

FIG. 1. Charge-sensing-based readout of a charge qubit. (a) A double-dot charge qubit is read out by a quantum point contact (QPC). (b) QPC current is modeled as a sequence of indirect measurements via another qubit (the meter), with basis states $|B\rangle$ and $|T\rangle$. The meter is Coulomb coupled to dot R of the charge qubit with interaction strength $\delta\gamma$, hence the probability of tunneling through the meter depends on the charge qubit state.

similar negative effects. We compare the QMQ model to earlier approaches [64–68] in SM S7 [69].

We consider the setup shown in Fig. 1(a). The charge qubit is formed by a single carrier in the DQD; the qubit basis states $|L\rangle$ and $|R\rangle$ correspond to its position. The QPC current is high (low) if the DQD charge is in the left (right) dot, due to Coulomb repulsion between the DQD charge and QPC electrons. In our QMQ model, the QPC is also represented by a single-carrier DQD, see Fig. 1(b), with basis states corresponding to the bottom ($|B\rangle$) and top ($|T\rangle$) dots.

The Hamiltonian of the qubit-meter system reads

$$\hat{H}_{\mathrm{tot}} = \hat{H}_{\mathrm{charge}} + \hat{H}_{\mathrm{m}} + \hat{H}^{\mathrm{c}}_{\mathrm{int}}, \tag{1}$$

where $\hat{H}_{\mathrm{charge}} = \epsilon\hat{\sigma}_z + t\hat{\sigma}_x$, $\hat{H}_{\mathrm{m}} = \gamma\hat{\tau}_x$, $\hat{H}^{\mathrm{c}}_{\mathrm{int}} = -\delta\gamma|R\rangle\langle R|\hat{\tau}_x$, $\hat{\sigma}_z = |L\rangle\langle L| - |R\rangle\langle R|$, $\hat{\sigma}_x = |L\rangle\langle R| + |R\rangle\langle L|$, and $\hat{\tau}_x = |T\rangle\langle B| + |B\rangle\langle T|$. Furthermore, 2ϵ is the on-site energy detuning, t is the tunneling amplitude of the qubit, γ is the tunneling amplitude of the meter, and the interaction strength $\delta\gamma$ describes the Coulomb repulsion between the qubit and the meter.

One way to operate the charge qubit [70,71] is to perform coherent control at $t > 0$ and $\epsilon = 0$, and sweep ϵ and t to a readout point with $\epsilon \gg t$ [72]. Then, readout in the basis of the ground $|\mathrm{g}\rangle$ and excited $|\mathrm{e}\rangle$ states (at the readout point) is carried out by measuring the QPC current and inferring binary value g or e from the current trace.

The QMQ model describes the process of reading out the qubit state ρ_{pre}. The readout is modeled as a sequence of indirect measurements, each consisting of three steps: (1) The meter is initialized in state $|B\rangle$. This state represents an electron approaching the QPC from the bottom lead. (2) The qubit-meter system evolves unitarily according to $\hat{H}_{\mathrm{tot}}$ for time $\Delta\tau$, entangling data and meter qubits via the interaction $\hat{H}^{\mathrm{c}}_{\mathrm{int}}$. The meter's tunneling rate γ and the time step $\Delta\tau$ are set such that by time $\Delta\tau$, the transition probability to state $|T\rangle$ is $1/2$ in an equal superposition or mixture of $|L\rangle$ and $|R\rangle$. This corresponds to a QPC tuned to its charge-sensing working point where its conductance is $1/2$ of the conductance quantum. (3) The meter is measured projectively in the $\{|B\rangle, |T\rangle\}$ basis. The assigned measurement outcome is the number of transmitted electrons, i.e., 0 (1) if the QPC electron is found in the bottom (top) dot.

The number $N \gg 1$ of these indirect measurements corresponds to the number of electrons attempting to transit the QPC during readout. The current flowing through the QPC is represented as an N-long bitstring, which contains 1-s where the QPC electron was transmitted. The state of the qubit is inferred from the transmission ratio $k = N_{\mathrm{t}}/N$ using the maximum-likelihood principle, where N_{t} is the number of electrons transmitted. That is, we infer e if the probability of obtaining the measured transmission ratio is greater for the initial state $|\mathrm{e}\rangle$ then for $|\mathrm{g}\rangle$; we infer g otherwise.

Measurement and backaction—The quantum channels corresponding to the final outcomes e and g are represented by superoperators $\mathcal{M}_{\mathrm{e}}$ and $\mathcal{M}_{\mathrm{g}}$. They are called *measurement operations* [62,73], and they map the premeasurement state to the unnormalized postmeasurement state conditional on the outcome. In the QMQ model, these measurement operations can be efficiently computed numerically (see SM S1 E [69]). Since $\mathcal{M}_{\mathrm{g}}$ and $\mathcal{M}_{\mathrm{e}}$ completely characterize the measurement, we extract all relevant readout metrics from them.

Infidelity is expressed with the measurement operations as

$$1 - \mathcal{F} \equiv 1 - \frac{1}{2}(\mathrm{Tr}\{\mathcal{M}_{\mathrm{e}}[|\mathrm{e}\rangle\langle\mathrm{e}|]\} + \mathrm{Tr}\{\mathcal{M}_{\mathrm{g}}[|\mathrm{g}\rangle\langle\mathrm{g}|]\}). \tag{2}$$

Figure 2(a) shows the infidelity as a function of integration time $\tau_{\mathrm{int}} = N\Delta\tau$. For short integration times, the infidelity decreases with increasing τ_{int}, since we gain more information about the initial state. For $t = 0$, the infidelity vanishes as $\tau_{\mathrm{int}} \to \infty$. However, for $t \neq 0$, the infidelity increases after an ideal integration time τ_{id}. As argued below, this increase is due to measurement backaction leading to qubit relaxation.

The time dependence of the infidelity in Fig. 2(a) is explained as follows. The pace of information gain upon readout is quantified by the measurement rate Γ_{m}, i.e., the decay rate of the overlap between the two distributions of the transmission ratio k corresponding to premeasurement states $|\mathrm{g}\rangle$ and $|\mathrm{e}\rangle$. This overlap has the form $1 - \Phi(\sqrt{2\Gamma_{\mathrm{m}}\tau_{\mathrm{int}}})$, through which Γ_{m} is defined, where Φ is the cumulative distribution function of the normal distribution. Upon calculating Γ_{m} up to lowest (zeroth) order in t/ϵ (see SM S3 [69]), which is the relevant limit at the readout point, we find

$$\Gamma_{\mathrm{m}} = \frac{1}{2}\left(\frac{\delta\gamma}{\hbar}\right)^2 \Delta\tau. \tag{3}$$

This rate characterizes the decrease of the infidelity in Fig. 2(a) for short integration times.

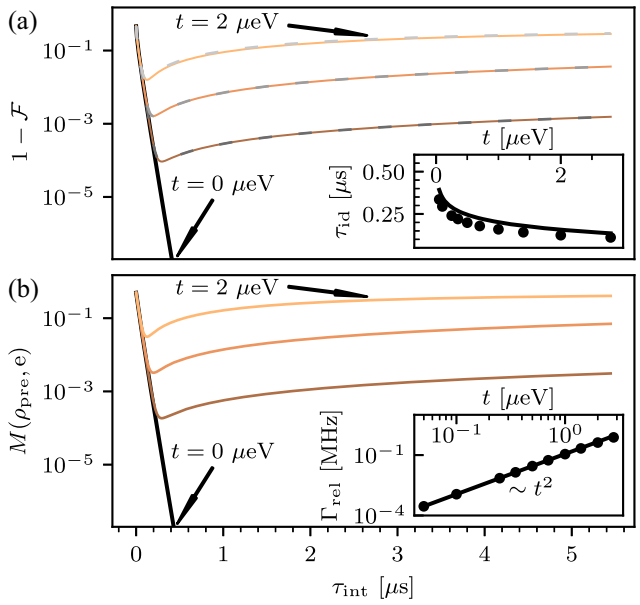

FIG. 2. Measurement benchmarks for charge qubit readout. (a) Infidelity. The continuous lines show the numerical values of infidelity. The dashed lines show an analytical estimate of the infidelity (see SM S5 [69], which relies on Ref. [74]). Inset: optimal integration time determined from exact numerical calculations (dots) and analytical estimate (line) (see SM S5 [69]). (b) Mixedness calculated numerically for $\rho_{pre} = (|e\rangle\langle e| + |g\rangle\langle g|)/2$ and outcome e. Inset: relaxation rate from numerical (dots) and analytical (line) calculations. We used the following parameters for the plots: $\epsilon = 10$ μeV, $\gamma = 5$ μeV, $\delta\gamma = 0.5$ μeV, $\Delta\tau = 0.11$ ns. The latter three values correspond to experimentally realistic current values (SM S2 [69]). The values of the residual tunneling used are $t \in \{0, 0.1, 0.5, 2\}$ μeV.

A nonzero residual tunneling $t > 0$ implies $[\hat{H}_{charge}, \hat{H}^{c}_{int}] \neq 0$. This, in turn, implies readout backaction in the form of qubit relaxation [64,75] characterized by the relaxation rate Γ^{c}_{rel}, which we express (see SM S4 [69]) as

$$\Gamma^{c}_{rel} = \frac{1}{2}\frac{t^2\delta\gamma^2}{\epsilon^4\Delta\tau}\sin^2\left(\frac{\epsilon\Delta\tau}{\hbar}\right). \tag{4}$$

This rate quantifies the speed at which the unconditional postmeasurement state $\mathcal{M}[\rho_{in}] = \mathcal{M}_g[\rho_{in}] + \mathcal{M}_e[\rho_{in}]$ approaches the completely mixed state. The inset of Fig. 2(b) shows that Eq. (4) (solid line) matches the relaxation rates obtained numerically (points) for the investigated parameter range. Note that Eq. (4) is not valid if the argument of the sine is close to $n\pi$, $n \in \mathbb{Z}^+$ (see SM S4 [69]).

The second readout metric we consider is the mixedness of the postmeasurement state. In a projective measurement of a qubit, the postmeasurement state is pure. However, in our setup, the postmeasurement state is mixed, except for the special case $t = 0$ and $\tau_{int} \to \infty$. The postmeasurement state depends on the premeasurement state ρ_{pre} and the measurement outcome $r \in \{e, g\}$. We express the postmeasurement state mixedness with the measurement operations as

$$M(\rho_{pre}, r) \equiv 1 - \mathrm{Tr}\{\rho^2_{post,r}\}, \tag{5}$$

with the conditional postmeasurement state $\rho_{post,r} = \mathcal{M}_r[\rho_{pre}]/\mathrm{Tr}\{\mathcal{M}_r[\rho_{pre}]\}$. A nonzero mixedness indicates deviations from a projective measurement. In Fig. 2(b), the mixedness for outcome $r = e$ is shown for the fully mixed premeasurement state, as a function of integration time. The qualitative dependence of the mixedness on integration time is similar to that of the infidelity, and is well described by the measurement and relaxation rates.

These results confirm that a residual tunneling degrades readout, making precise control of t essential. Below, we argue that the same conclusion applies for Pauli-blockade-based spin qubit readout.

Spin qubit—Spin qubit readout often relies on Pauli blockade spin-to-charge conversion and subsequent charge sensing [27–29]. We generalize the QMQ model to describe this readout. We focus on Pauli-blockade readout of a single-electron (Loss-DiVincenzo [1]) spin qubit. This requires a DQD with a target spin to be measured in, say, the right dot and a known reference spin in the left dot, see Fig. 3(a). Readout is done in three steps: spin-to-charge conversion, charge sensing, and charge-to-spin conversion. Without relaxation processes, this readout is nondestructive.

We model the two-electron DQD by the Hamiltonian of a two-site Hubbard model:

$$\hat{H}_{spin} = \hat{H}_{on\text{-}site} + \hat{H}_{tun} + \hat{H}_{Zeeman} + \hat{H}_{Coulomb}, \tag{6}$$

where $\hat{H}_{on\text{-}site} = \epsilon/2\sum_s(\hat{n}_{L,s} - \hat{n}_{R,s})$, $\hat{H}_{tun} = t\sum_s\left(\hat{a}^\dagger_{R,s}\hat{a}_{L,s} + \text{H.c.}\right)$, $\hat{H}_{Zeeman} = Z_L/2(\hat{n}_{L\uparrow} - \hat{n}_{L\downarrow}) + Z_R/2(\hat{n}_{R\uparrow} - \hat{n}_{R\downarrow})$, $\hat{H}_{Coulomb} = U(\hat{n}_{L,\uparrow}\hat{n}_{L,\downarrow} + \hat{n}_{R,\uparrow}\hat{n}_{R,\downarrow})$, $\hat{a}^\dagger_{\sigma,s}$ is an electronic creation operator on dot $\sigma \in \{L, R\}$ with spin $s \in \{\uparrow, \downarrow\}$, and $\hat{n}_{\sigma,s} = \hat{a}^\dagger_{\sigma,s}\hat{a}_{\sigma,s}$. Furthermore, $Z_\sigma = \mu_B g_\sigma B_z$ is the Zeeman energy in dot σ due to a magnetic field B, proportional to the g factor g_σ of dot σ, and U is the Coulomb repulsion energy between two electrons occupying the same dot. At this point, spin-orbit interaction is included in Eq. (6) by considering different g factors in the two dots.

For later use, we introduce the six two-electron basis states $|S_{(0,2)}\rangle = \hat{a}^\dagger_{R\uparrow}\hat{a}^\dagger_{R\downarrow}|0\rangle$, $|\uparrow\downarrow\rangle = \hat{a}^\dagger_{L\uparrow}\hat{a}^\dagger_{R\downarrow}|0\rangle$, etc, with $|0\rangle$ denoting the state of the empty DQD. These states are eigenstates of $\hat{H}_{spin}$ at $t = 0$. The detuning dependence of the five lowest-energy states for $t = 0$ is illustrated in Fig. 3(d) as the dashed lines. We focus on readout errors due to the backaction of the charge sensor. Therefore, we assume perfect state transfer during spin-to-charge and charge-to-spin conversion between the computational states

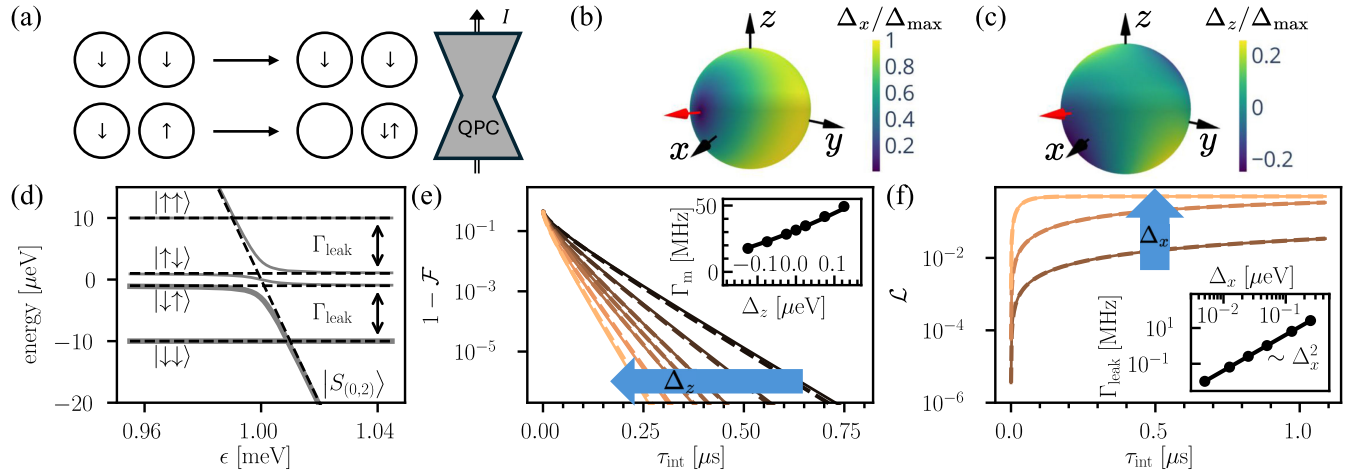

FIG. 3. Spin-qubit readout error due to g-tensor modulation by the charge sensor. (a) Readout setup in a double quantum dot: Spin in the right dot is to be read out utilizing the reference spin in the left dot, with the combination of Pauli spin blockade and charge sensing. (b),(c) Readout sweet spot, shown by red arrow: magnetic field direction providing optimized readout ($\Delta_x = 0$), for g-tensor parameters from Ref. [76]. Colors show normalized Δ_x (b) and Δ_z (c) as functions of the magnetic field direction. The normalization factor $\Delta_{\max}$ is the maximum of Δ_x as a function of magnetic field direction. (d) Lowest five energy levels of the double dot as a function of detuning for $t = 0$ (dashed black lines) and $t = 2$ μeV (gray solid lines), for $U = 1$ meV, $Z_L = 11$ μeV, and $Z_R = 9$ μeV. Arrows indicate incoherent QPC-induced transitions activated by a nonzero Δ_x. (e) Readout infidelity for $\Delta_x = 0$ and $\Delta_z \in \{-0.125, -0.075, -0.025, 0, 0.025, 0.075, 0.125\}$ μeV. Arrow indicates increasing Δ_z. Inset: analytical (solid) and numerical (dots) results for the measurement rate Γ_m as function of Δ_z. (f) Leakage from the initial state $|\downarrow\downarrow\rangle$ for $\Delta_z = 0$ and for $\Delta_x \in \{0.0125, 0.05, 0.25\}$ μeV. Arrow indicates increasing Δ_x. Inset: analytical (solid) and numerical (dots) results for the relaxation rate Γ_{leak} as a function of Δ_x. Parameters for (e),(f): $\epsilon = U + 40$ μeV, $t = 0$ μeV, $\gamma = 5$ μeV, $\delta\gamma = 0.5$ μeV, U, Z_L, Z_R as above.

at the operational point [left end of Fig. 3(d)] and the computational states at the readout point [right end of Fig. 3(d)] according to, say, $|\downarrow\uparrow\rangle \leftrightarrow |S_{0,2}\rangle$ and $|\downarrow\downarrow\rangle \leftrightarrow |\downarrow\downarrow\rangle$.

The interaction between the DQD and the QPC is described by the term

$$\hat{H}^{\text{s}}_{\text{int}} = -\delta\gamma |S_{(0,2)}\rangle\langle S_{(0,2)}| \otimes \hat{\tau}_x, \tag{7}$$

which is a natural generalization of $\hat{H}^{\text{c}}_{\text{int}}$ in Eq. (1). This $\hat{H}^{\text{s}}_{\text{int}}$ captures that the transmission probability of the QPC is lower if there are two electrons in the right dot, instead of one.

We use this model to describe readout of the spin qubit in dot R. The measurement operations $\mathcal{M}_\downarrow$ and $\mathcal{M}_\uparrow$ are computed analogously to those of the charge qubit readout as a function of model parameters.

Ideally, tunnel coupling is switched off at the readout position during charge sensing. State-of-the-art device fabrication makes this possible [29], and shuttling in a sparse dot array [6] provides an alternative solution. However, in a given device, it might be impossible to set $t = 0$, e.g., due to the gate electrode geometry, or gate-voltage constraints. This enhances readout errors, akin to the case of the charge qubit discussed above. A small but nonzero residual tunneling fulfilling $t \ll \epsilon - U$ and $4t^2/(\epsilon - U) \ll |Z_L - Z_R|$ implies that $|S_{(0,2)}\rangle$ is slightly hybridized with $|\uparrow\downarrow\rangle$ and $|\downarrow\uparrow\rangle$; the perturbed eigenstates are denoted by $|\tilde{S}_{(0,2)}\rangle$, $|\tilde{\uparrow\downarrow}\rangle$, and $|\tilde{\downarrow\uparrow}\rangle$. Consequently, the interaction of the DQD with the QPC electrons leads to incoherent transitions between the state $|\tilde{S}_{(0,2)}\rangle$ and the states $|\tilde{\uparrow\downarrow}\rangle$ and $|\tilde{\downarrow\uparrow}\rangle$. The measurement benchmarks infidelity and mixedness show the same qualitative behavior as illustrated in Fig. 2 for the charge qubit. This backaction is discussed further in SM S6 [69].

From now on, we assume that the tunnel coupling can be switched off ($t = 0$). In this case, another mechanism affecting readout is the spin-orbit mediated interaction between the DQD spins and the fluctuating electric field created by the QPC electrons [76–80], often described as g-tensor modulation. To account for this, we generalize the interaction Hamiltonian of Eq. (7) as

$$\hat{H}^{\text{s}}_{\text{int}} = -(\delta\gamma |S_{(0,2)}\rangle\langle S_{(0,2)}| + \hat{\mathbf{s}}_R \cdot \boldsymbol{\Delta}) \otimes \hat{\tau}_x, \tag{8}$$

where $\boldsymbol{\Delta} = \mu_{\text{B}} g'_R \mathbf{B}/2$ describes the spin-charge coupling, i.e., change of the g tensor on dot R caused by the electric field of the charges flowing through the QPC. Here, g'_R is a 3×3 real matrix, and $\hat{\mathbf{s}}_R$ represents the spin vector on the right dot, e.g., $\hat{s}_{R,z} = \hat{n}_{R\uparrow} - \hat{n}_{R\downarrow}$. The joint Hamiltonian of the system and the meter is given by Eq. (6), Eq. (8) with $t = 0$, and $\hat{H}_{\text{m}}$ in Eq. (1).

First, we discuss Zeeman field modulation perpendicular to the static field, i.e., $\boldsymbol{\Delta} = (\Delta_x, 0, 0)$. In this case $[H_{\text{spin}}, H^{\text{s}}_{\text{int}}] \neq 0$, leading to leakage from the computational

state $|\downarrow\downarrow\rangle$ to the state $|\downarrow\uparrow\rangle$, which is outside of the computational subspace (see SM S4 [69]). The leakage probability for a premeasurement state ρ_{pre} of the computational subspace $\mathrm{span}(\{|\downarrow\downarrow\rangle, |S_{(0,2)}\rangle\})$ at the readout point is expressed as

$$\mathcal{L}(\rho_{\mathrm{pre}}) = \mathrm{Tr}(P_{\mathrm{leak}}\mathcal{M}[\rho_{\mathrm{pre}}]), \tag{9}$$

where $\mathcal{M} = \mathcal{M}_{\downarrow} + \mathcal{M}_{\uparrow}$, and $P_{\mathrm{leak}} = 1 - |\downarrow\downarrow\rangle\langle\downarrow\downarrow| - |S_{(0,2)}\rangle\langle S_{(0,2)}|$.

Of the two computational basis states, $|S_{(0,2)}\rangle$ is not prone to readout-induced leakage, but $|\downarrow\downarrow\rangle$ is. Numerical results for leakage from $|\downarrow\downarrow\rangle$ are shown with solid lines in Fig. 3(f). Longer integration times lead to increased leakage, saturating at $\mathcal{L}(\tau_{\mathrm{int}} \to \infty) = 1/2$; increasing the coupling strength Δ_x also increases leakage. Analytical derivations (SM S4 [69]) for this case show that leakage can be expressed as $\mathcal{L}(|\downarrow\downarrow\rangle) = (1 - e^{-\Gamma_{\mathrm{leak}}\tau})/2$, with the leakage rate

$$\Gamma_{\mathrm{leak}} = \frac{8\Delta_x^2}{Z_R^2\Delta\tau}\sin^2\left(\frac{Z_R\Delta\tau}{2\hbar}\right). \tag{10}$$

This analytical result for the leakage is shown in Fig. 3(f) as dashed lines, matching the numerical results well. This leakage mechanism, although undesired as it corrupts the postmeasurement state, does not affect the readout infidelity, as the sensor does not differentiate between $|\downarrow\downarrow\rangle$ and $|\downarrow\uparrow\rangle$.

Second, we discuss Zeeman field modulation parallel to the static field, i.e., $\boldsymbol{\Delta} = (0, 0, \Delta_z)$. Then, it holds that $[\hat{H}_{\mathrm{spin}}, \hat{H}^{\mathrm{s}}_{\mathrm{int}}] = 0$, hence, there is no relaxation or leakage, and the infidelity goes to zero as $\tau_{\mathrm{int}} \to \infty$. This is shown numerically in Fig. 3(e), as the solid lines. Figure 3(e) also reveals that for a given integration time, infidelity decreases and hence readout improves as Δ_z is increased. This improvement is due to the spin-charge coupling term of Eq. (8), which, in this special case, makes the QPC current dependent on $\hat{s}_{R,z}$ and hence facilitates readout. This is explained by expressing $\hat{H}^{\mathrm{s}}_{\mathrm{int}}$ in the two-dimensional computational subspace, resulting in $-(\delta\gamma + \Delta_z)|S_{(0,2)}\rangle\langle S_{(0,2)}|$, up to a global energy shift. Therefore, we substitute $\delta\gamma \to \delta\gamma + \Delta_z$ in Eq. (3), and conclude that Γ_{m} shows an approximately linear dependence on Δ_z for $\Delta_z \ll \delta\gamma$. This is confirmed by the inset of Fig. 3(e), where the above analytical approximation (solid) is compared to results (dots) obtained by fitting the function $1 - \Phi(\sqrt{2\Gamma_{\mathrm{m}}\tau_{\mathrm{int}}})$ on the infidelity data in Fig. 3(e).

The above results imply that leakage is eliminated in a magnetic field configuration where the static Zeeman field in dot R is parallel to the local Zeeman field fluctuation caused the QPC. Interestingly, this can be achieved for any generic g tensor and g' matrix: the equation $g\mathbf{B} \| g'\mathbf{B}$ for the unknown $\mathbf{B}$ is solved by the right eigenvectors of $g^{-1}g'$, and the latter 3×3 matrix has either 1 or 3 real eigenvalue-eigenvector pairs, which describe physical magnetic-field directions [81]. In the case of 3 real eigenvectors, it is optimal to orient the magnetic field along that of the greatest eigenvalue, to maximize the measurement rate Γ_{m}. The above consideration identifies a readout sweet spot in terms of the magnetic-field direction, akin to dephasing and relaxation sweet spots identified earlier [81–87]. The red arrows in Figs. 3(b) and 3(c) show the readout sweet spot for a the g-tensor and g-tensor modulation g' from Ref. [76], for which there is a single real eigenvalue of $g^{-1}g'$. In a multiqubit device, *in situ* tuning of the g-tensor parameters by gate voltages [76,82,86,88–96] could be used to synchronize the readout sweet spots (see also discussion in SM S9 [69]). We propose to find the readout sweet spot device configuration by measuring the leakage probability, as described in SM S8 [69].

Conclusions—We have identified two readout error sources for quantum-dot-based charge and spin qubits: residual tunneling and g-tensor modulation. We have characterized the parameter dependence of these errors via a minimal model of the readout process, going beyond readout infidelity, describing postmeasurement state mixedness and leakage—key benchmarks for protocols recycling qubits. Our results provide clear guidelines to optimize readout by controlling the tunnel coupling and exploiting magnetic readout sweet spots, and pave the way for understanding and minimizing measurement errors across a variety of charge-sensing techniques.

Acknowledgments—We thank Gy. Frank, B. Kolok, R. Németh, Sudipto Das, E. G. Kelly, and P. Harvey-Collard for fruitful discussions. This work was supported by the Ministry of Culture and Innovation and the National Research, Development and Innovation Office within the Quantum Information National Laboratory of Hungary, Grant No. 2022-2.1.1-NL-2022-00004 (D. S., G. S., and A. P.); via the EKÖP_KDP-24-1-BME-2 funding scheme through Project No. 2024-2.1.2-EKÖP-KDP-2024-00005 (D. S. and A. P.); and by the European Union within the Horizon Europe research and innovation programme via the projects IGNITE (D. S. and A. P.), ONCHIPS (D. S. and A. P.), and QLSI2 (D. S., S. B., and A. P.). This work was supported by the HUN-REN Hungarian Research Network through the Supported Research Groups Programme, No. HUN-REN-BME-BCE Quantum Technology Research Group (No. TKCS-2024/34). G. S. was supported by the János Bolyai Research Scholarship of the Hungarian Academy of Science. B. H., S. B., and D. L. also acknowledge support from NCCR Spin (Grant No. 225153) and the NCCR Spin Mobility Grant. S. B. was sponsored in part by the Army Research Office, Award No. W911NF-23-1-0110.

The views and conclusions contained in this document are those of the authors and should not be interpreted as representing the official policies, either expressed or

implied, of the Army Research Office or the U.S. Government. The U.S. Government is authorized to reproduce and distribute reprints for Government purposes notwithstanding any copyright notation herein.

Data availability—The data that support the findings of this article are openly available [97].

[1] D. Loss and D. P. DiVincenzo, Phys. Rev. A **57**, 120 (1998).
[2] R. Hanson, L. P. Kouwenhoven, J. R. Petta, S. Tarucha, and L. M. K. Vandersypen, Rev. Mod. Phys. **79**, 1217 (2007).
[3] F. A. Zwanenburg, A. S. Dzurak, A. Morello, M. Y. Simmons, Lloyd C. L. Hollenberg, G. Klimeck, S. Rogge, S. N. Coppersmith, and M. A. Eriksson, Rev. Mod. Phys. **85**, 961 (2013).
[4] M. Eriksson, M. Friesen, S. Coppersmith, R. Joynt, L. Klein, K. Slinker, C. Tahan, P. Mooney, J. Chu, and S. Koester, Quantum Inf. Process. **3**, 133 (2004).
[5] G. Burkard, T. D. Ladd, A. Pan, J. M. Nichol, and J. R. Petta, Rev. Mod. Phys. **95**, 025003 (2023).
[6] C.-A. Wang, V. John, H. Tidjani, C. X. Yu, A. S. Ivlev, C. Déprez, F. van Riggelen-Doelman, B. D. Woods, N. W. Hendrickx, W. I. L. Lawrie, L. E. A. Stehouwer, S. D. Oosterhout, A. Sammak, M. Friesen, G. Scappucci, S. L. de Snoo, M. Rimbach-Russ, F. Borsoi, and M. Veldhorst, Science **385**, 447 (2024).
[7] X. Zhang, E. Morozova, M. Rimbach-Russ, D. Jirovec, T.-K. Hsiao, P. C. Fariña, C.-A. Wang, S. D. Oosterhout, A. Sammak, G. Scappucci, M. Veldhorst, and L. M. K. Vandersypen, Nat. Nanotechnol. **20**, 209 (2025).
[8] S. G. J. Philips, M. T. Mądzik, S. V. Amitonov, S. L. de Snoo, M. Russ, N. Kalhor, C. Volk, W. I. L. Lawrie, D. Brousse, L. Tryputen, B. P. Wuetz, A. Sammak, M. Veldhorst, G. Scappucci, and L. M. K. Vandersypen, Nature (London) **609**, 919 (2022).
[9] N. W. Hendrickx, W. I. L. Lawrie, M. Russ, F. van Riggelen, S. L. de Snoo, R. N. Schouten, A. Sammak, G. Scappucci, and M. Veldhorst, Nature (London) **591**, 580 (2021).
[10] C. Kloeffel and D. Loss, Annu. Rev. Condens. Matter Phys. **4**, 51 (2013).
[11] L. M. K. Vandersypen, H. Bluhm, J. S. Clarke, A. S. Dzurak, R. Ishihara, A. Morello, D. J. Reilly, L. R. Schreiber, and M. Veldhorst, npj Quantum Inf. **3**, 34 (2017).
[12] G. Scappucci, C. Kloeffel, F. A. Zwanenburg, D. Loss, M. Myronov, J.-J. Zhang, S. D. Franceschi, G. Katsaros, and M. Veldhorst, Nat. Rev. Mater. **6**, 926 (2021).
[13] P. Stano and D. Loss, Nat. Rev. Phys. **4**, 672 (2022).
[14] R. Maurand, X. Jehl, D. Kotekar-Patil, A. Corna, H. Bohuslavskyi, R. Laviéville, L. Hutin, S. Barraud, M. Vinet, M. Sanquer, and S. De Franceschi, Nat. Commun. **7**, 13575 (2016).
[15] X. Xue *et al.*, Nature (London) **593**, 205 (2021).
[16] D. Jirovec, A. Hofmann, A. Ballabio, P. M. Mutter, G. Tavani, M. Botifoll, A. Crippa, J. Kukucka, O. Sagi, F. Martins, J. Saez-Mollejo, I. Prieto, M. Borovkov, J. Arbiol, D. Chrastina, G. Isella, and G. Katsaros, Nat. Mater. **20**, 1106 (2021).
[17] S. D. Liles, D. J. Halverson, Z. Wang, A. Shamim, R. S. Eggli, I. K. Jin, J. Hillier, K. Kumar, I. Vorreiter, M. J. Rendell, J. Y. Huang, C. C. Escott, F. E. Hudson, W. H. Lim, D. Culcer, A. S. Dzurak, and A. R. Hamilton, Nat. Commun. **15**, 7690 (2024).
[18] L. C. Camenzind, S. Geyer, A. Fuhrer, R. J. Warburton, D. M. Zumbühl, and A. V. Kuhlmann, Natl. Electron. Rev. **5**, 178 (2022).
[19] A. M. J. Zwerver *et al.*, Natl. Electron. Rev. **5**, 184 (2022).
[20] S. Neyens *et al.*, Nature (London) **629**, 80 (2024).
[21] S. Geyer, B. Hetényi, S. Bosco, L. C. Camenzind, R. S. Eggli, A. Fuhrer, D. Loss, R. J. Warburton, D. M. Zumbühl, and A. V. Kuhlmann, Nat. Phys. **20**, 1152 (2024).
[22] P. Steinacker *et al.*, Nature (London) **646**, 81 (2025).
[23] X. Xue, M. Russ, N. Samkharadze, B. Undseth, A. Sammak, G. Scappucci, and L. M. K. Vandersypen, Nature (London) **601**, 343 (2022).
[24] A. Noiri, K. Takeda, T. Nakajima, T. Kobayashi, A. Sammak, G. Scappucci, and S. Tarucha, Nature (London) **601**, 338 (2022).
[25] A. R. Mills, C. R. Guinn, M. J. Gullans, A. J. Sigillito, M. M. Feldman, E. Nielsen, and J. R. Petta, Sci. Adv. **8**, eabn5130 (2022).
[26] K. Takeda, A. Noiri, T. Nakajima, L. C. Camenzind, T. Kobayashi, A. Sammak, G. Scappucci, and S. Tarucha, npj Quantum Inf. **10**, 22 (2024).
[27] P. Harvey-Collard, B. D'Anjou, M. Rudolph, N. T. Jacobson, J. Dominguez, G. A. Ten Eyck, J. R. Wendt, T. Pluym, M. P. Lilly, W. A. Coish, M. Pioro-Ladrière, and M. S. Carroll, Phys. Rev. X **8**, 021046 (2018).
[28] J. Z. Blumoff *et al.*, PRX Quantum **3**, 010352 (2022).
[29] M. Nurizzo, B. Jadot, P.-A. Mortemousque, V. Thiney, E. Chanrion, D. Niegemann, M. Dartiailh, A. Ludwig, A. D. Wieck, C. Bäuerle, M. Urdampilleta, and T. Meunier, PRX Quantum **4**, 010329 (2023).
[30] F. Vigneau, F. Fedele, A. Chatterjee, D. Reilly, F. Kuemmeth, M. F. Gonzalez-Zalba, E. Laird, and N. Ares, Appl. Phys. Rev. **10**, 021305 (2023).
[31] L. Pereira, J. J. García-Ripoll, and T. Ramos, Phys. Rev. Lett. **129**, 010402 (2022).
[32] L. Pereira, J. J. García-Ripoll, and T. Ramos, npj Quantum Inf. **9**, 22 (2023).
[33] K. Rudinger, G. J. Ribeill, Luke C. G. Govia, M. Ware, E. Nielsen, K. Young, T. A. Ohki, R. Blume-Kohout, and T. Proctor, Phys. Rev. Appl. **17**, 014014 (2022).
[34] Z. Zhang, S. Chen, Y. Liu, and L. Jiang, PRX Quantum **6**, 010310 (2025).
[35] J. Hines and T. Proctor, Phys. Rev. Lett. **134**, 020602 (2025).
[36] D. Hothem, J. Hines, C. Baldwin, D. Gresh, R. Blume-Kohout, and T. Proctor, arXiv:2410.16706.
[37] D. McLaren, M. A. Graydon, A. A. Mahmoud, and J. J. Wallman, arXiv:2502.00179.
[38] K. C. Miao *et al.*, Nat. Phys. **19**, 1780 (2023).
[39] M. McEwen *et al.*, Nat. Commun. **12**, 1761 (2021).
[40] F. Battistel, B. M. Varbanov, and B. M. Terhal, PRX Quantum **2**, 030314 (2021).
[41] J. F. Marques, H. Ali, B. M. Varbanov, M. Finkel, H. M. Veen, S. L. M. van der Meer, S. Valles-Sanclemente, N. Muthusubramanian, M. Beekman, N. Haider, B. M. Terhal, and L. DiCarlo, Phys. Rev. Lett. **130**, 250602 (2023).

[42] M. Liepelt, T. Peduzzi, and J. R. Wootton, J. Phys. A **57**, 255302 (2024).
[43] G. P. Gehér, M. Jastrzebski, E. T. Campbell, and O. Crawford, npj Quantum Inf. **11**, 39 (2025).
[44] C. Tornow, N. Kanazawa, W. E. Shanks, and D. J. Egger, Phys. Rev. Appl. **17**, 064061 (2022).
[45] E. Bäumer, V. Tripathi, D. S. Wang, P. Rall, E. H. Chen, S. Majumder, A. Seif, and Z. K. Minev, PRX Quantum **5**, 030339 (2024).
[46] A. Fleury, J. Brown, E. Lloyd, M. Hernandez, and I. H. Kim, J. Chem. Theory Comput. **20**, 10807 (2024).
[47] J. P. T. Stenger, G. Bazargan, N. T. Bronn, and D. Gunlycke, arXiv:2504.15187.
[48] E. Bäumer, V. Tripathi, A. Seif, D. Lidar, and D. S. Wang, arXiv:2403.09514.
[49] C. Cao and J. Eisert, arXiv:2505.04705.
[50] K. Ono, D. G. Austing, Y. Tokura, and S. Tarucha, Science **297**, 1313 (2002).
[51] J. R. Petta, A. C. Johnson, J. M. Taylor, E. A. Laird, A. Yacoby, M. D. Lukin, C. M. Marcus, M. P. Hanson, and A. C. Gossard, Science **309**, 2180 (2005).
[52] F. H. L. Koppens, C. Buizert, K. J. Tielrooij, I. T. Vink, K. C. Nowack, T. Meunier, L. P. Kouwenhoven, and L. M. K. Vandersypen, Nature (London) **442**, 766 (2006).
[53] S. Haldar, M. Munk, H. Havir, W. Khan, S. Lehmann, C. Thelander, K. A. Dick, P. Samuelsson, P. P. Potts, and V. F. Maisi, Phys. Rev. Lett. **134**, 023601 (2025).
[54] D. Taubert, M. Pioro-Ladrière, D. Schröer, D. Harbusch, A. S. Sachrajda, and S. Ludwig, Phys. Rev. Lett. **100**, 176805 (2008).
[55] M. S. Ferguson, L. C. Camenzind, C. Müller, D. E. F. Biesinger, C. P. Scheller, B. Braunecker, D. M. Zumbühl, and O. Zilberberg, arXiv:2010.04635.
[56] C. E. Young and A. A. Clerk, Phys. Rev. Lett. **104**, 186803 (2010).
[57] J. M. Elzerman, R. Hanson, J. S. Greidanus, L. H. Willems van Beveren, S. De Franceschi, L. M. K. Vandersypen, S. Tarucha, and L. P. Kouwenhoven, Phys. Rev. B **67**, 161308 (R) (2003).
[58] J. M. Elzerman, R. Hanson, L. H. Willems van Beveren, B. Witkamp, L. M. K. Vandersypen, and L. P. Kouwenhoven, Nature (London) **430**, 431 (2004).
[59] S. Gustavsson, R. Leturcq, B. Simovič, R. Schleser, T. Ihn, P. Studerus, K. Ensslin, D. C. Driscoll, and A. C. Gossard, Phys. Rev. Lett. **96**, 076605 (2006).
[60] M. Reznikov, M. Heiblum, H. Shtrikman, and D. Mahalu, Phys. Rev. Lett. **75**, 3340 (1995).
[61] T. Muro, Y. Nishihara, S. Norimoto, M. Ferrier, T. Arakawa, K. Kobayashi, T. Ihn, C. Rössler, K. Ensslin, C. Reichl, and W. Wegscheider, Phys. Rev. B **93**, 195411 (2016).
[62] H. M. Wiseman and G. J. Milburn, *Quantum Measurement and Control* (Cambridge University Press, Cambridge, England, 2009).
[63] L. Diosi, *A Short Course in Quantum Information Theory: An Approach From Theoretical Physics*, Lecture Notes in Physics (Springer, Berlin, Heidelberg, 2007).
[64] H.-S. Goan, G. J. Milburn, H. M. Wiseman, and H. B. Sun, Phys. Rev. B **63**, 125326 (2001).
[65] H.-S. Goan and G. J. Milburn, Phys. Rev. B **64**, 235307 (2001).
[66] R. Landauer, IBM J. Res. Dev. **1**, 223 (1957).
[67] M. Büttiker, Phys. Rev. Lett. **57**, 1761 (1986).
[68] Y. Blanter and M. Büttiker, Phys. Rep. **336**, 1 (2000).
[69] See Supplemental Material at http://link.aps.org/supplemental/10.1103/4x97-np1f for derivation of analytical results, description of our simulation method, comparison with previous work, and a proposal for measuring back-action induced leakage and discussion.
[70] K. D. Petersson, J. R. Petta, H. Lu, and A. C. Gossard, Phys. Rev. Lett. **105**, 246804 (2010).
[71] P. Scarlino, J. H. Ungerer, D. J. van Woerkom, M. Mancini, P. Stano, C. Müller, A. J. Landig, J. V. Koski, C. Reichl, W. Wegscheider, T. Ihn, K. Ensslin, and A. Wallraff, Phys. Rev. X **12**, 031004 (2022).
[72] C. V. Meinersen, S. Bosco, and M. Rimbach-Russ, Eur. Phys. J. Quantum Technol. **12**, 125 (2025).
[73] A. Hashim, L. B. Nguyen, N. Goss, B. Marinelli, R. K. Naik, T. Chistolini, J. Hines, J. P. Marceaux, Y. Kim, P. Gokhale, T. Tomesh, S. Chen, L. Jiang, S. Ferracin, K. Rudinger, T. Proctor, K. C. Young, R. Blume-Kohout, and I. Siddiqi, PRX Quantum **6**, 030202 (2025).
[74] R. Pyke, J. R. Stat. Soc. Ser. B **27**, 395 (2018).
[75] M. Boissonneault, J. M. Gambetta, and A. Blais, Phys. Rev. A **79**, 013819 (2009).
[76] A. Crippa, R. Maurand, L. Bourdet, D. Kotekar-Patil, A. Amisse, X. Jehl, M. Sanquer, R. Laviéville, H. Bohuslavskyi, L. Hutin, S. Barraud, M. Vinet, Y.-M. Niquet, and S. De Franceschi, Phys. Rev. Lett. **120**, 137702 (2018).
[77] Y. Kato, R. C. Myers, D. C. Driscoll, A. C. Gossard, J. Levy, and D. D. Awschalom, Science **299**, 1201 (2003).
[78] M. Borhani, V. N. Golovach, and D. Loss, Phys. Rev. B **73**, 155311 (2006).
[79] B. Venitucci, L. Bourdet, D. Pouzada, and Y.-M. Niquet, Phys. Rev. B **98**, 155319 (2018).
[80] S. Studenikin, M. Korkusinski, M. Takahashi, J. Ducatel, A. Padawer-Blatt, A. Bogan, D. G. Austing, L. Gaudreau, P. Zawadzki, A. Sachrajda, Y. Hirayama, L. Tracy, J. Reno, and T. Hargett, Commun. Phys. **2**, 159 (2019).
[81] A. Sen, G. Frank, B. Kolok, J. Danon, and A. Pályi, Phys. Rev. B **108**, 245406 (2023).
[82] N. Piot, B. Brun, V. Schmitt, S. Zihlmann, V. P. Michal, A. Apra, J. C. Abadillo-Uriel, X. Jehl, B. Bertrand, H. Niebojewski, L. Hutin, M. Vinet, M. Urdampilleta, T. Meunier, Y.-M. Niquet, R. Maurand, and S. D. Franceschi, Nat. Nanotechnol. **17**, 1072 (2022).
[83] V. P. Michal, J. C. Abadillo-Uriel, S. Zihlmann, R. Maurand, Y.-M. Niquet, and M. Filippone, Phys. Rev. B **107**, L041303 (2023).
[84] L. Mauro, E. A. Rodríguez-Mena, M. Bassi, V. Schmitt, and Y.-M. Niquet, Phys. Rev. B **109**, 155406 (2024).
[85] S. Bosco and D. Loss, Phys. Rev. Lett. **127**, 190501 (2021).
[86] S. Bosco, B. Hetényi, and D. Loss, PRX Quantum **2**, 010348 (2021).
[87] O. Malkoc, P. Stano, and D. Loss, Phys. Rev. Lett. **129**, 247701 (2022).
[88] N. W. Hendrickx, L. Massai, M. Mergenthaler, F. J. Schupp, S. Paredes, S. W. Bedell, G. Salis, and A. Fuhrer, Nat. Mater. **23**, 920 (2024).

[89] V. John, C. X. Yu, B. van Straaten, E. A. Rodríguez-Mena, M. Rodríguez, S. Oosterhout, L. E. A. Stehouwer, G. Scappucci, S. Bosco, M. Rimbach-Russ, Y.-M. Niquet, F. Borsoi, and M. Veldhorst, Nat. Commun. **16**, 10560 (2025).
[90] M. Rimbach-Russ, V. John, B. van Straaten, and S. Bosco, Phys. Rev. Lett. **135**, 197001 (2025).
[91] S. Bosco, P. Scarlino, J. Klinovaja, and D. Loss, Phys. Rev. Lett. **129**, 066801 (2022).
[92] S. Bosco, M. Benito, C. Adelsberger, and D. Loss, Phys. Rev. B **104**, 115425 (2021).
[93] J. Saez-Mollejo, D. Jirovec, Y. Schell, J. Kukucka, S. Calcaterra, D. Chrastina, G. Isella, M. Rimbach-Russ, S. Bosco, and G. Katsaros, arXiv:2408.03224.
[94] M. J. Carballido, S. Svab, R. S. Eggli, T. Patlatiuk, P. C. Kwon, J. Schuff, R. M. Kaiser, L. C. Camenzind, A. Li, N. Ares, E. P. A. M. Bakkers, S. Bosco, J. C. Egues, D. Loss, and D. M. Zumbühl, Nat. Commun. **16**, 7616 (2025).
[95] M. Bassi, E.-A. Rodrıguez-Mena, B. Brun, S. Zihlmann, T. Nguyen, V. Champain, J. C. Abadillo-Uriel, B. Bertrand, H. Niebojewski, R. Maurand, Y.-M. Niquet, X. Jehl, S. D. Franceschi, and V. Schmitt, Nat. Phys. **22**, 75 (2026).
[96] I. Seidler, B. Hetényi, L. Sommer, L. Massai, K. Tsoukalas, E. G. Kelly, A. Orekhov, M. Aldeghi, S. W. Bedell, S. Paredes, F. J. Schupp, M. Mergenthaler, G. Salis, A. Fuhrer, and P. Harvey-Collard, arXiv:2510.03125.
[97] D. Svastits, 10.5281/zenodo.16024845 (2025).